

The B_s and D_s decay constants in 3 flavor lattice QCD

Matthew Wingate,^{1,2} Christine T. H. Davies,³ Alan Gray,^{3,1} G. Peter Lepage,⁴ and Junko Shigemitsu¹

¹*Department of Physics, The Ohio State University, Columbus, OH 43210, USA*

²*Institute for Nuclear Theory, University of Washington, Seattle, WA 98195-1550, USA*

³*Department of Physics & Astronomy, University of Glasgow, Glasgow, G12 8QQ, UK*

⁴*Laboratory of Elementary Particle Physics, Cornell University, Ithaca, NY 14853, USA*

(Dated: 13 November 2018)

Capitalizing on recent advances in lattice QCD, we present a calculation of the leptonic decay constants f_{B_s} and f_{D_s} that includes effects of one strange sea quark and two light sea quarks. The discretization errors of improved staggered fermion actions are small enough to simulate with 3 dynamical flavors on lattices with spacings around 0.1 fm using present computer resources. By shedding the quenched approximation and the associated lattice scale ambiguity, lattice QCD greatly increases its predictive power. NRQCD is used to simulate heavy quarks with masses between $1.5m_c$ and m_b . We arrive at the following results: $f_{B_s} = 260 \pm 7 \pm 26 \pm 8 \pm 5$ MeV and $f_{D_s} = 290 \pm 20 \pm 29 \pm 29 \pm 6$ MeV. The first quoted error is the statistical uncertainty, and the rest estimate the sizes of higher order terms neglected in this calculation. All of these uncertainties are systematically improvable by including another order in the weak coupling expansion, the nonrelativistic expansion, or the Symanzik improvement program.

PACS numbers: 12.38.Gc, 13.20.Fc, 13.20.He

We present the first complete calculation of the B_s and D_s decay constants with 3 flavors of sea quarks with small masses. The D_s decay constant, f_{D_s} , has been measured [1, 2], and CLEO-c promises to reduce the experimental errors significantly. The comparison of experimental and lattice results will be a vital test of lattice QCD. The B_s and B_d decay constants, f_{B_s} and f_B , are necessary in order to constrain V_{td} via $\bar{B}^0 - B^0$ mixing. Since experimental measurements of f_{B_s} remain elusive, an accurate lattice calculation is critical for improving phenomenological tests of CKM unitarity.

The calculation presented below makes use of lattice Monte Carlo simulations, done by the MILC collaboration [3], which include the proper sea quark content: one dynamical strange quark and two flavors of dynamical quarks with masses as light as $m_s/4$. The correct number of flavors is necessary in order for the lattice theory to have the same β -function as real QCD. Only then can we expect, in principle, lattice results to agree with experimental measurements.

Inclusion of light up and down sea quarks is essential for accurate lattice phenomenology. The innovation which allows this on present computers is an improved staggered discretization of the light quark action [4, 5, 6, 7, 8, 9, 10, 11]. For each dynamical flavor the fourth root of the fermion determinant is used in the Monte Carlo updating algorithm. Despite some open theoretical issues concerning staggered fermion algorithms, these calculations are free of ambiguities present in quenched simulations, provided the u and d sea quark masses are light enough. In practice, calculations involving unstable particles or multi-hadronic final states require new or refined techniques before they can be reliably simulated; however, there are several quantities for which numerical calculation is

straightforward. Ref. [12] presents lattice results for a variety of these “gold-plated” quantities, including f_π and f_K , and several splittings in the Υ spectrum. The change from $n_f = 0$ results, which differ substantially from experiment, to $n_f = 3$ results, which agree with experiment up to the 3% lattice uncertainties, suggests that the improved staggered fermion method correctly simulates QCD. Heavy-light pseudoscalar leptonic decay constants, presented here, fit into the “gold-plated” category [12].

Our calculation of f_{B_s} and f_{D_s} uses standard lattice QCD methods. Correlation functions were computed using a subset of gauge field configurations generated by the MILC collaboration. The configurations include the effects of 2 dynamical light quarks with equal bare mass, denoted by m_ℓ^{sea} , and 1 dynamical strange quark, with bare mass m_s^{sea} . The lattices we used have spacings of about 1/8 fm and volumes of about $(2.5 \text{ fm})^3 \times 8.0 \text{ fm}$. We focus on the configurations where $m_\ell^{\text{sea}}/m_s^{\text{sea}} = 1/5$ and $2/5$. As we discuss below, the physical strange quark mass, m_s , obtained from the light hadron spectrum is actually $4/5$ of m_s^{sea} , so the light sea quark masses are approximately $m_s/4$ and $m_s/2$.

Details of the Monte Carlo simulations which generated the ensemble of gauge fields are given in [3]. In this work we use a level splitting in the Υ spectrum, e.g. the $\Upsilon(2S - 1S)$ splitting, to determine the lattice spacing, instead of the length scale r_1 , derived from the static quark potential, which was used in [3]. The Υ spectrum will be presented in detail in a future publication [13]; however, we note here that as the light sea quark mass is increased, the $\Upsilon(1P - 1S)$ splitting becomes slightly smaller than experiment when the lattice spacing is set by $\Upsilon(2S - 1S)$. With statistical errors between 1 – 2%, the difference between experiment and lattice values for the $1P - 1S$ splitting is 0σ , 1σ , and 2σ for $m_\ell^{\text{sea}}/m_s \approx$

TABLE I: Heavy quark parameters and meson masses for two values of the light sea quark mass.

aM_0	n	$m_\ell^{\text{sea}} \approx m_s/4$ (568 config)		$m_\ell^{\text{sea}} \approx m_s/2$ (468 config)	
		$m_{H_s}^{\text{kin}}$ (GeV)	$m_{H_s}^{\text{pert}}$ (GeV)	$m_{H_s}^{\text{kin}}$ (GeV)	$m_{H_s}^{\text{pert}}$ (GeV)
2.8	2	5.6(2)	5.3(4)	5.22(17)	5.4(4)
2.1	4	4.38(10)	4.2(3)	4.28(11)	4.3(3)
1.6	4	3.52(6)	3.5(3)	3.56(7)	3.5(3)
1.2	6	2.84(5)	2.78(19)	2.93(4)	2.83(19)
1.0	6	2.53(4)	2.41(16)	2.60(3)	2.45(16)

1/4, 1/2, and 3/4, respectively. Except for estimating sea quark mass effects, we use the $m_\ell^{\text{sea}}/m_s \approx 1/4$ lattice to obtain our results.

The analysis of [3] has also been updated with respect to determining the quark mass corresponding to the physical strange quark mass sector. Rather than using $\bar{s}s$ mesons which are either unstable (the ϕ) or do not exist (the pseudoscalar) we use the results of the partially quenched chiral perturbation theory analysis of m_K and m_π [12, 14]. On lattices with $au_0m_\ell^{\text{sea}} = 0.007, 0.01$, and 0.02, the physical strange sector is obtained with $au_0m_s^{\text{val}} = 0.040$. (Here we keep explicit a factor of the mean-link u_0 , which was absorbed into the definition of the light bare quark mass in [3].)

Table I lists the bare heavy quark masses used in this work, along with the corresponding NRQCD stabilization parameter n . For each mass, we estimate the heavy-light meson mass two ways: the “kinetic mass” $m_{H_s}^{\text{kin}}$ is extracted from finite momentum correlators using the meson dispersion relation, and the “perturbative mass” $m_{H_s}^{\text{pert}}$ is estimated from the zero momentum correlator and the one-loop heavy quark mass renormalization. We find that the bare heavy quark mass $aM_0 = 2.8$ produces the correct experimental mass for the Υ [15] and the B_s within statistical errors.

When we construct correlation functions for heavy-light mesons, we use the equivalence between staggered and naive fermion propagators. The operators we use are the same ones as with Wilson-like discretizations or in the continuum limit. This method for computing the B_s mass and decay constant has been presented, along with tests on quenched lattices, in recent work [16].

The B_s decay constant is defined through the axial vector matrix element; $\langle 0|A_\mu|B_s(p_\mu)\rangle = f_{B_s}p_\mu$. Here we use only the temporal component. Up through $O(1/M_0)$ three lattice operators contribute to A_0 , the leading-order current, J_0 , and two sub-leading currents J_1 and J_2 ; the matching from the lattice to the continuum is done in perturbation theory [17]. A one-loop calculation yields

$$A_0 = (1 + \alpha_s \tilde{\rho}_0)J_0^{(0)} + (1 + \alpha_s \rho_1)J_0^{(1,\text{sub})} + \alpha_s \rho_2 J_0^{(2,\text{sub})} \quad (1)$$

where $J_0^{(1,\text{sub})} = J_0^{(1)} - \alpha_s \zeta_{10} J_0^{(0)}$, and so too for $J_0^{(2,\text{sub})}$.

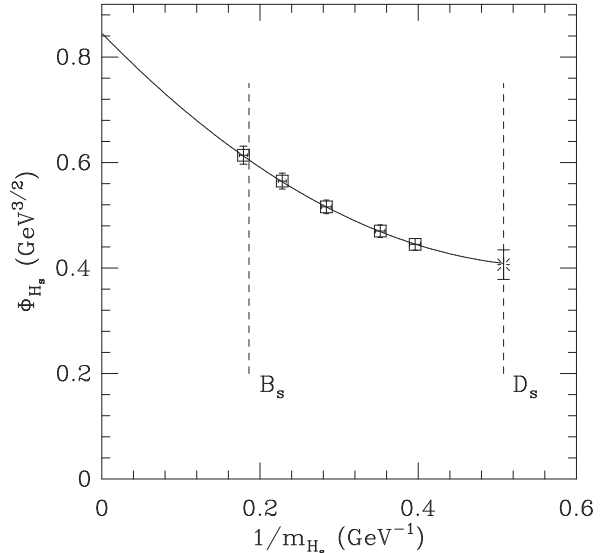


FIG. 1: Squares show $\Phi_{H_s} \equiv f_{H_s} \sqrt{m_{H_s}}$ vs. $1/m_{H_s}$ on the $m_\ell^{\text{sea}}/m_s \approx 1/4$ lattice. The solid line shows the fit described in the text, and the asterisk shows the value of Φ_{H_s} extrapolated to the charm sector. Experimental values for $1/m_{B_s}$ and $1/m_{D_s}$ are shown as dashed vertical lines.

These operators explicitly subtract, through one-loop, the power-law mixing of $J_0^{(0)}$ with $J_0^{(1)}$ and $J_0^{(2)}$ [18]. The perturbative calculation which determines $\tilde{\rho}_0, \rho_1, \rho_2, \zeta_{10}$, and ζ_{20} will be presented separately [19].

From fits to correlation functions, we extract the combination $\Phi_{H_s} \equiv f_{H_s} \sqrt{m_{H_s}}$. Let us denote by $\Phi^{(i)}$ the contribution of $J_0^{(i)}$ to Φ_{H_s} . For this calculation the matrix elements are computed for mesons at rest, so $\Phi^{(1)} = \Phi^{(2)}$. Table II summarizes fits to the numerical data, converted to physical units using $1/a = 1.59(2)$ GeV for the $m_\ell^{\text{sea}} \approx m_s/4$ lattice and $1/a = 1.61(2)$ GeV for the $m_\ell^{\text{sea}} \approx m_s/2$ lattice. (The quoted uncertainties come from statistical and fitting uncertainties in the $\Upsilon(2S - 1S)$ splitting [13].) By comparing $\Phi^{(1)}/\Phi^{(0)}$ with $\Phi^{(1,\text{sub})}/\Phi^{(0)}$ one can observe the sizable power law mixing of $J^{(0)}$ with $J^{(1)}$. The expression (1) absorbs the mixing back into the term proportional to $J^{(0)}$, so $\Phi^{(1,\text{sub})}/\Phi^{(0)}$ represents the physical contribution of $1/M_0$ terms to Φ_{H_s} up to two-loop corrections. The 4% contribution from the $1/M_0$ operator we see for the B_s ($aM_0 = 2.8$) is the same size seen in quenched studies over a range of lattice spacings [18].

Figure 1 shows the heavy quark mass dependence of Φ_{H_s} on m_{H_s} (plotted as squares). The data are fit well by

$$\Phi_{H_s} = \Phi_{H_s}^{\text{stat}} \left(1 + \frac{C_1}{m_{H_s}} + \frac{C_2}{m_{H_s}^2} \right) \quad (2)$$

with a correlated χ^2 per degree-of-freedom of 0.7/2. We

TABLE II: Simulation results for $\Phi_{H_s} \equiv f_{H_s} \sqrt{m_{H_s}}$ for each light sea quark mass and heavy quark mass. The third column lists the leading order term $\Phi^{LO} \equiv (1 + \alpha_s \tilde{\rho}_0) \Phi^{(0)}$, The fourth and fifth columns show the contributions of $J_0^{(1)}$, with respect to $\Phi^{(0)}$, before and after the power law subtraction. The sixth column gives the result for Φ_{H_s} . Statistical and fitting uncertainties are quoted in parentheses (not including the statistical uncertainty in $1/a$).

$m_{\tilde{t}}^{\text{sea}}/m_s \approx 1/4$					
aM_0	$\Phi^{LO} (\text{GeV}^{3/2})$	$\Phi^{(1)}/\Phi^{(0)}$	$\Phi^{(1,\text{sub})}/\Phi^{(0)}$	$\Phi_{H_s} (\text{GeV}^{3/2})$	
2.8	0.640(11)	-9.0(4) %	-3.7(4) %	0.614(13)	
2.1	0.598(10)	-11.7(4) %	-5.0(4) %	0.565(11)	
1.6	0.557(8)	-14.7(4) %	-6.4(4) %	0.516(9)	
1.2	0.519(7)	-18.3(4) %	-7.8(4) %	0.470(8)	
1.0	0.499(6)	-20.7(4) %	-8.6(4) %	0.445(7)	
$m_{\tilde{t}}^{\text{sea}}/m_s \approx 1/2$					
aM_0	$\Phi^{LO} (\text{GeV}^{3/2})$	$\Phi^{(1)}/\Phi^{(0)}$	$\Phi^{(1,\text{sub})}/\Phi^{(0)}$	$\Phi_{H_s} (\text{GeV}^{3/2})$	
2.8	0.640(15)	-8.9(6) %	-3.6(6) %	0.615(14)	
2.1	0.599(11)	-11.4(6) %	-4.7(6) %	0.567(12)	
1.6	0.563(7)	-14.2(5) %	-5.9(5) %	0.523(9)	
1.2	0.528(6)	-17.7(5) %	-7.1(5) %	0.481(6)	
1.0	0.510(6)	-20.0(5) %	-7.9(5) %	0.459(6)	

find $\Phi_{H_s}^{\text{stat}} = 0.85(4) \text{ GeV}^{3/2}$, $C_1 = -1.82(20) \text{ GeV}$, and $C_2 = 1.59(35) \text{ GeV}^2$. It is important to note that most of the mass dependence of Φ_{H_s} comes through the action and not through the $1/M_0$ currents. A fit to the leading order $\Phi^{LO} \equiv (1 + \alpha_s \tilde{\rho}_0) \Phi^{(0)}$ (Table II) yields similar fit parameters: $\Phi^{\text{stat},LO} = 0.83(4) \text{ GeV}^{3/2}$, $C_1^{LO} = -1.53(19) \text{ GeV}$, and $C_2^{LO} = 1.32(32) \text{ GeV}^2$. Since the action is responsible for most of the m_{H_s} dependence and is accurate through $O(\Lambda_{\text{QCD}}^2/m_Q^2)$, performing the operator matching through $O(1/M_0^2)$ should yield only small corrections to the values for $\Phi_{H_s}^{\text{stat}}$, C_1 , and C_2 listed above.

We use the fit above to interpolate Φ_{H_s} slightly to the physical value of $1/m_{B_s}$. The result is $f_{B_s} = 260(7) \text{ MeV}$, where the quoted statistical error combines statistical errors from $1/a$ and $a^{3/2}\Phi_{B_s}$. Uncertainties in $m_{H_s}^{\text{kin}}$ are small compared to the other uncertainties in the fit. The systematic uncertainties due to the neglect of higher order terms are estimated by assuming coefficients of $O(1)$. For example, two-loop terms omitted in (1) are estimated to be 10% effects, taking the coupling constant defined through the plaquette $\alpha_s = \alpha_P^{n_f=3}(2/a) = 0.32$ [20]. This is the largest systematic uncertainty. Leading discretization errors are $O(\alpha_s a^2 \Lambda_{\text{QCD}}^2)$, where Λ_{QCD} is the typical scale of nonperturbative dynamics. Taking $1/a = 1.6 \text{ GeV}$ and $\Lambda_{\text{QCD}} = 400 \text{ MeV}$ implies 2% cutoff effects. The operator matching neglects terms $O(\Lambda_{\text{QCD}}^2/m_b^2)$ or approximately 1%. We note that the coefficient of the spin-dependent term in the action is the tree level one,

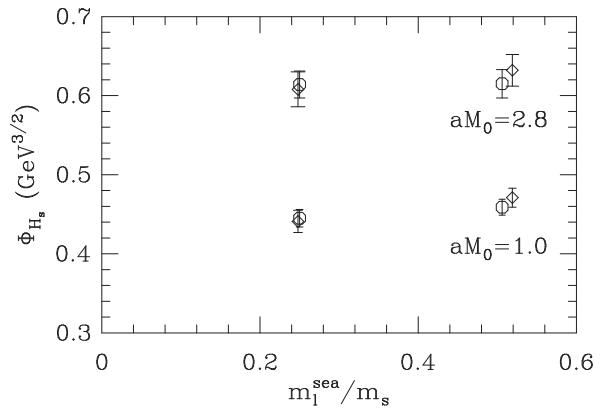


FIG. 2: Dependence of Φ_{H_s} on the light sea quark mass. The upper data points correspond to the B_s ($aM_0 = 2.8$) and the lower points come from our lightest heavy quark mass, $aM_0 = 1.0$. The different symbols indicate which quantity was used to set the lattice spacing: octagons use the $\Upsilon(2S - 1S)$ splitting and diamonds use the $\Upsilon(1P - 1S)$ splitting. Error bars represent combined statistical uncertainties of $1/a$ and $a^{3/2}\Phi_{H_s}$.

giving rise to an $O(\alpha_s \Lambda_{\text{QCD}}/m_Q)$ error in the action, which is about 3% for bottom quarks. This does not necessarily translate into a comparably large error in decay constants where the spin dependence is not obvious; however, to be conservative, we quote an overall 3% uncertainty due to relativistic corrections.

Extrapolating the fit described above to the physical value for $1/m_{D_s}$ requires care since higher order terms in $1/m_{H_s}$ become increasingly important. The fit above extrapolates to $f_{D_s} = 290(10) \text{ MeV}$. We use a Bayesian analysis to estimate possible effects due to higher order terms. Allowing terms like $C_n/m_{H_s}^n$ with $n \geq 3$ in the fit (2), with Gaussian priors for $C_n/\text{GeV}^n = 0 \pm \delta$ and $\delta = 1 - 4$, we find higher order terms could lead to a 20 MeV error in f_{D_s} . This is taken as the statistical and fitting uncertainty. The $O(\alpha_s^2)$ perturbative error and the $O(\alpha_s a^2 \Lambda_{\text{QCD}}^2)$ discretization error are again estimated to be 10% and 2%, respectively. For charmed mesons $\Lambda_{\text{QCD}}/m_c = 1/4$, so the $O(\Lambda_{\text{QCD}}^2/m_Q^2)$ corrections to the matching are estimated to be 6%. As mentioned above, the $O(\alpha_s \Lambda_{\text{QCD}}/m_Q)$ error in the spin dependent term in the action probably does not lead to a proportional error in the decay constant. Nevertheless, we quote 10% as a conservative estimate of possible relativistic corrections.

Figure 2 shows Φ_{H_s} vs. light sea quark mass for two heavy quark masses. We show the results where the lattice spacing is set from the $\Upsilon(2S - 1S)$ splitting and the same data adjusted as if the spacing were set from the $\Upsilon(1P - 1S)$ splitting. No sea quark mass dependence is observed for $aM_0 = 2.8$, nor is a significant dependence observed for $aM_0 = 1.0$ when the spacing is set with $\Upsilon(2S - 1S)$. Only because there is a 2% ambiguity in

setting the scale with $m_l^{\text{sea}} \approx m_s/2$ does there appear to be some sea quark mass effect in the $aM_0 = 1.0$ data with the $\Upsilon(1P - 1S)$ spacing. No such scale setting ambiguity exists for the data with $m_l^{\text{sea}} \approx m_s/4$, which is where our main results are obtained.

Experimental measurements of the leptonic decay constants for B_s and D_s are challenging, so these are rare cases where lattice QCD can lead experiment. The most recent and precise experimental results for f_{D_s} are $280 \pm 17 \pm 25 \pm 34$ MeV [1] and $285 \pm 19 \pm 40$ MeV [2], which agree well with the calculation presented here. Shrinking the experimental uncertainties on f_{D_s} is a major goal of the CLEO-c program.

Turning to comparison with the existing literature on lattice QCD, we quote recent world averages and comment on another new result. The $n_f = 3$ results presented here have central values larger than lattice calculations with $n_f = 0$ or 2. For example, recent averages [21] of quenched results are $f_{B_s}^{n_f=0} = 200(20)$ MeV and $f_{D_s}^{n_f=0} = 230(14)$ MeV, significantly lower than our results. The 2 flavor world averages, $f_{B_s}^{n_f=2} = 230(30)$ MeV and $f_{D_s}^{n_f=2} = 250(30)$ MeV, are higher than the quenched and agree within the quoted uncertainties.

Recently the JLQCD collaboration reported a lattice result using two dynamical flavors of improved Wilson fermions with mass between $0.7m_s$ and $2.9m_s$ [22]. They quote $f_{B_s} = 215(9)_{(-2)}^{(+0)}(13)_{(-0)}^{(+6)}$ MeV, with the first error statistical, second from chiral extrapolation of the sea quark mass, third from finite lattice spacing combined with truncation of NRQCD and perturbative expansions, and the fourth from ambiguity in setting the strange quark mass. This calculation uses much larger quark masses than ours, uses unstable hadron masses to set the lattice spacing and m_s , and does not include a dynamical strange quark. Further work will be required to determine which, if any, of these accounts for the differences with our results. For instance, it would be interesting to calculate a^{-1} from several Υ splittings on the configurations of [22] and compare f_{B_s} using those scales to the value quoted in their paper, which uses the scale set by m_ρ .

Recent sum rule calculations agree within errors for the B_s decay constant: e.g. $f_{B_s}^{\text{s.r.}} = 236(30)$ MeV [23, 24]. On the other hand, they do not calculate an increase in the decay constant as the heavy quark mass decreases: e.g. $f_{D_s}^{\text{s.r.}} = 235(24)$ MeV [24].

To summarize, we have completed a calculation of the B_s and D_s decay constants using 3 flavor lattice QCD. The more realistic sea quark content allows a unique lattice spacing to be determined using one of several quantities [12], enabling more reliable prediction of quantities not yet measured experimentally. Our final results are

$$\begin{aligned} f_{B_s} &= 260 \pm 7 \pm 26 \pm 8 \pm 5 \text{ MeV} \\ f_{D_s} &= 290 \pm 20 \pm 29 \pm 29 \pm 6 \text{ MeV}. \end{aligned} \quad (3)$$

The uncertainties quoted are respectively due to statistics and fitting, perturbation theory, relativistic corrections, and discretization effects. The result for the D_s decay constant agrees with experimental determinations, and the result for the B_s decay constant is a prediction for future experiments. Improvement of the lattice results requires a two-loop perturbative matching calculation or the use of fully nonperturbative methods. On the other hand, much of the perturbative uncertainty cancels in the ratio f_{B_s}/f_{B_d} . Work is underway to study f_{B_d} using the methods discussed in this paper [25].

Simulations were performed at NERSC. We thank the MILC collaboration for their gauge field configurations. This work was supported in part by the DOE, NSF, PPARC, and the EU.

-
- [1] M. Chadha *et al.* (CLEO), Phys. Rev. **D58**, 032002 (1998).
 - [2] A. Heister *et al.* (ALEPH), Phys. Lett. **B528**, 1 (2002).
 - [3] C. W. Bernard *et al.*, Phys. Rev. **D64**, 054506 (2001).
 - [4] C. W. Bernard *et al.*, Nucl. Phys. Proc. Suppl. **60A**, 297 (1998).
 - [5] G. P. Lepage, Nucl. Phys. Proc. Suppl. **60A**, 267 (1998), hep-lat/9707026.
 - [6] C. W. Bernard *et al.* (MILC), Phys. Rev. **D58**, 014503 (1998), hep-lat/9712010.
 - [7] G. P. Lepage, Phys. Rev. **D59**, 074502 (1999), hep-lat/9809157.
 - [8] K. Orginos and D. Toussaint (MILC), Phys. Rev. **D59**, 014501 (1999), hep-lat/9805009.
 - [9] D. Toussaint and K. Orginos (MILC), Nucl. Phys. Proc. Suppl. **73**, 909 (1999), hep-lat/9809148.
 - [10] K. Orginos, D. Toussaint, and R. L. Sugar (MILC), Phys. Rev. **D60**, 054503 (1999), hep-lat/9903032.
 - [11] C. Bernard *et al.* (MILC), Phys. Rev. **D61**, 111502 (2000), hep-lat/9912018.
 - [12] C. T. H. Davies *et al.* (HPQCD, MILC, FNAL) (2003), hep-lat/0304004.
 - [13] A. Gray *et al.*, in preparation.
 - [14] C. Aubin *et al.* (2002), hep-lat/0209066.
 - [15] A. Gray *et al.* (HPQCD) (2002), hep-lat/0209022.
 - [16] M. Wingate, J. Shigemitsu, C. T. H. Davies, G. P. Lepage, and H. D. Trotter, Phys. Rev. **D67**, 054505 (2003).
 - [17] C. J. Morningstar and J. Shigemitsu, Phys. Rev. **D57**, 6741 (1998).
 - [18] S. Collins, C. Davies, J. Hein, G. P. Lepage, C. J. Morningstar, J. Shigemitsu, and J. H. Sloan, Phys. Rev. **D63**, 034505 (2001).
 - [19] E. Gulez, J. Shigemitsu, and M. Wingate (in preparation).
 - [20] C. Davies *et al.* (2002), hep-lat/0209122.
 - [21] S. M. Ryan, Nucl. Phys. Proc. Suppl. **106**, 86 (2002).
 - [22] S. Aoki *et al.* (JLQCD) (2003), hep-ph/0307039.
 - [23] M. Jamin and B. O. Lange, Phys. Rev. **D65**, 056005 (2002).
 - [24] S. Narison, Phys. Lett. **B520**, 115 (2001).
 - [25] M. Wingate *et al.* (2003), hep-lat/0309092.